



Self-propelled Janus micromotors for pH-responsive release of small molecule drug

Tijana Maric^{a,b,1,*}, Sýlvía Atladóttir^{a,b,1}, Lasse Højlund Eklund Thamdrup^{a,b}, Oleksii Ilchenko^{a,b}, Mahdi Ghavami^{a,b}, Anja Boisen^{a,b}

^a The Danish National Research Foundation and Villum Foundation's Center for Intelligent Drug Delivery and Sensing Using Microcontainers and Nanomechanics (IDUN), Denmark

^b Department of Health Technology, DTU Health Tech, Technical University of Denmark, 2800 Kgs., Lyngby, Denmark

ARTICLE INFO

Article history:

Received 6 December 2021

Revised 28 January 2022

Accepted 4 February 2022

Keywords:

Micromotors
Janus particles
Furosemide
CARS imaging
polymer coating
Eudragit

ABSTRACT

Oral administration of drugs has received significant attention in the last 1, 2 decades, as it is the most comfortable and painless administration route, which leads to high patient compliance. Although oral delivery of drugs shows positive effects in patients, several hurdles must be overcome such as enzymatic degradation, large pH-variations found throughout the gastrointestinal (GI) tract, and continuous mucus secretion. We have studied biocompatible non-toxic micromotors as promising man-made microdevices for targeted furosemide release. Micromotors are micro-scale autonomous entities that can perform various tasks in the GI tract as a result of their impressive motion abilities. Their directional motion makes them ideal candidates to bring the necessary drug dosage to where it is needed. **Herein, the micromotors were loaded for the first time with furosemide and coated with pH-sensitive polymer Eudragit® L100 using ultrasonic spray coating technique in order to achieve targeted drug delivery and pH-responsive release.** Coherent anti-Stokes Raman scattering spectroscopy (CARS) was used for visualizing drug loading efficiency on the surface of micromotors. *In vitro* drug release was evaluated under acidic and neutral pH chemical environments and obtained results confirm their function as pH-sensitive microdevices for a drug release.

© 2022 The Authors. Published by Elsevier Ltd.

This is an open access article under the CC BY license (<http://creativecommons.org/licenses/by/4.0/>)

1. Introduction

The work on novel delivery devices and concepts is attracting increased attention. Simultaneously, oral delivery is the preferred route of drug administration since it is minimum invasive and leads to high patient compliance [1]. Although oral delivery of drugs using traditional nano and microsystems [2–6] shows positive effects in patients with different diseases, several challenges must be addressed: the first pass-effect due to enzymatic degradation, large pH variations throughout the gastrointestinal (GI) tract, continuous mucus secretion, and poor permeability, as well as multiple chemical, enzymatic and physical barriers [7–9]. In order to reach the general systemic circulation, orally administered drugs

must first travel into the GI tract, adhere and penetrate through the mucus layer, transport across the epithelial barrier, infiltrate the hepatic portal vein and finally reach the general systemic circulation [10]. As a result, the oral bioavailability of many drugs is low, and novel micro-scale active carriers, such as micromotors, have been studied to improve bioavailability [11,12]. Recent innovations in nontoxic nano-materials and methods have led to the use of micromotors in biomedical applications [13,14]. In principle, micromotors are able to convert any type of received energy (chemical, magnetic, electric, ultrasound, thermal, light) into motion [15–17]. One key feature of these micromotors is their autonomous movement, which can improve the performance of drug carriers in the GI tract [18]. Micromotors can capture, transport, and release various cargo in different media. These attractive abilities make them capable of performing complex tasks, such as anti-cancer drug carrier [19], targeted drug delivery [20], microsurgeries [21], cancer therapies [22], biosensing [23], bioimaging [24], and separation of proteins and cells [25].

The group of J. Wang has studied the use of hydrogen bubble propelled micromotors extensively for many years. They have

* Corresponding author at: The Danish National Research Foundation and Villum Foundation's Center for Intelligent Drug Delivery and Sensing Using Microcontainers and Nanomechanics, Department of Health Technology, Technical University of Denmark, 2800 Kgs. Lyngby, Denmark.

E-mail address: tijma@dtu.dk (T. Maric).

¹ These authors contributed equally to this work.

fabricated micromotors loaded with multicomponent cargoes (SiO₂ and Au nanoparticles) that can be autonomously released followed by their self-destruction once their delivery mission has been completed [26]. Utilizing this combinational cargo delivery system could be beneficial for drug therapy that requires simultaneous administration of more than one drug. Biocompatible Janus CaCO₃/Au micromotors have been reported for targeted drug delivery of doxorubicin (DOX) and tumor treatment by combining thermophoretic and bubble propulsion mechanisms [11]. The same microparticles (CaCO₃) in cubical shapes coated with glucose oxidase (GOx) and Fe₃O₄ nanoparticles, were used as a double-engine microsystem for synergetic cancer treatment [27]. The enzymatic reaction of glucose oxidase in the presence of glucose acts as a chemical microsystem to enhance cellular uptake, whereas the addition of Fe₃O₄ nanoparticles enables magnetically guided targeting of cancer cells. Zhu et al. have fabricated micromotors from stable porous carbon nanocomposites and cobalt nanoparticles as carriers for DOX transportation and release [28].

Wang's group has shown that by incorporating a pH-sensitive enteric polymer (Eudragit® L100–55) into micromotors and tuning its thickness, micromotors can be successfully controlled to penetrate mucosal tissue along the gastrointestinal tract [29]. Uncoated micromotors showed significant retention and elimination in the stomach, micromotors with thin enteric coating were able to reach the duodenum, while micromotors with thick enteric coating travelled all the way to the ileum. In 2015, Gao et al. reported the first *in vivo* study of synthetic micromotors using a live mouse model [18]. Acid-powered PEDOT/Zn micromotors were propelled based on the self-propulsion bubble mechanism which led to significantly enhanced tissue penetration and retention in the stomach environment (compared to the static PEDOT/Pt micromotors) without causing any destructive effect on the gastric epithelial cells. The ability of the micromotors to self-destruct causes cargo payloads to be released autonomously and efficiently. This active micromotor-based delivery approach offers impressive improvement of orally administered cargoes compared to conventional passive diffusion [18].

Small molecule drugs such as furosemide currently suffer from relatively low bioavailability. Such drug could benefit from micromotor prompted delivery since this could facilitate higher uptake and thereby reduced drug dose (hereby reducing cost and potential side effects). Furosemide is a potent diuretic used to treat hypertension and edematous states related to hepatic, renal, and cardiac failure [30]. It is a class IV drug in Biopharmaceutical Classification System (BCS), meaning it has poor permeability and poor aqueous solubility; hence its oral bioavailability is relatively low [31]. It has been shown that the dosage form, presence of food, and underlying diseases can influence intestinal absorption, resulting in a highly variable bioavailability ranging from 20% to 60% [32].

In this study, we explored the possibility of delivering a small molecule drug at selective pH conditions, using micromotors and furosemide as our proof-of-concept drug. We developed self-propelled magnesium-gold (Mg-Au) micromotors, loaded them with furosemide and coated them with pH-sensitive polymer (Eudragit® L100) using ultrasonic spray coating technique. The respective micromotors are labelled based on the following compositions: magnesium-gold (Mg-Au), magnesium-gold-furosemide (Mg-Au-Furo), and magnesium-gold-furosemide-Eudragit®L100 (Mg-Au-Furo-Eudr). A conformal and protective Au shell was deposited using metal sputtering, leaving only a small opening to the underlying Mg where the particles were attached to a carrier substrate. Coherent anti-Stokes Raman scattering (CARS) microscopy was, to the best of our knowledge, used for the first time for characterization and imaging of drugs attached to the surface of micromotors. The autonomous propulsion and lifetime of the micromotors were tested in simulated intestinal media. Finally, we showed how

prepared Janus micromotors function as enterically coated self-propelled drug delivery devices by performing *in vitro* release studies in acidic and neutral (PBS) chemical environments.

2. Experimental section

2.1. Micromotors preparation

Magnesium (Mg) particles (TangShan WeiHao Magnesium Powder Co.; 20 ± 5 μm) were used as the base particles to prepare micromotors. 2 mg of the Mg particles were weighed and washed three times in acetone before use to minimize the presence of impurities and contaminants. The Mg particles were sonicated 3 times in a 2210 DTH Branson ultrasonic cleaner (Branson Ultrasonics, USA) for 10 min each time. The solution was centrifuged by 5430 Eppendorf microcentrifuge (Eppendorf, Germany) at 9000 rpm for 10 min after each washing step. 0.5 mL of the solution was dispersed onto a glass slide and dried at room temperature. The Mg particles were subsequently coated with an Au layer (layer thickness: 40 nm, sputtering time: 60 s, current: 40 mA, pressure: 0.1 mbar) using a Cressington 208HR (Cressington Scientific Instruments UK, Watford, England).

2.2. Drug loading and polymer coating

Next, a furosemide solution was prepared. 10 mg of furosemide (Fagron, Netherlands) was dissolved in 1 mL ethanol absolute (VWR, USA). Once the drug was fully dissolved, 0.5 mL of drug solution was dispersed over a glass slide, containing Mg-Au Janus micromotors and left to evaporate. Finally, the drug-loaded Mg-Au Janus micromotors were coated with Eudragit® L100 (Evonik Industries AG, Germany) solution (1% w/v in 2-propanol with DBS). An ultrasonic spray coater (ExacataCoat system from Sono-Tek, Milton NY, USA) equipped with an accumist nozzle was used to coat the micromotors. The flow rate, the generator power, the number of loops, and the cladding/shaping air pressure were 0.5 mL/min, 1.5 W, 2, and 0.02–0.03 bar, respectively. Alpha-Step IQ Stylus Profilometer (KLA-Tencor Corporation, Milpitas, USA) was used to measure the coating thickness of Eudragit® L100.

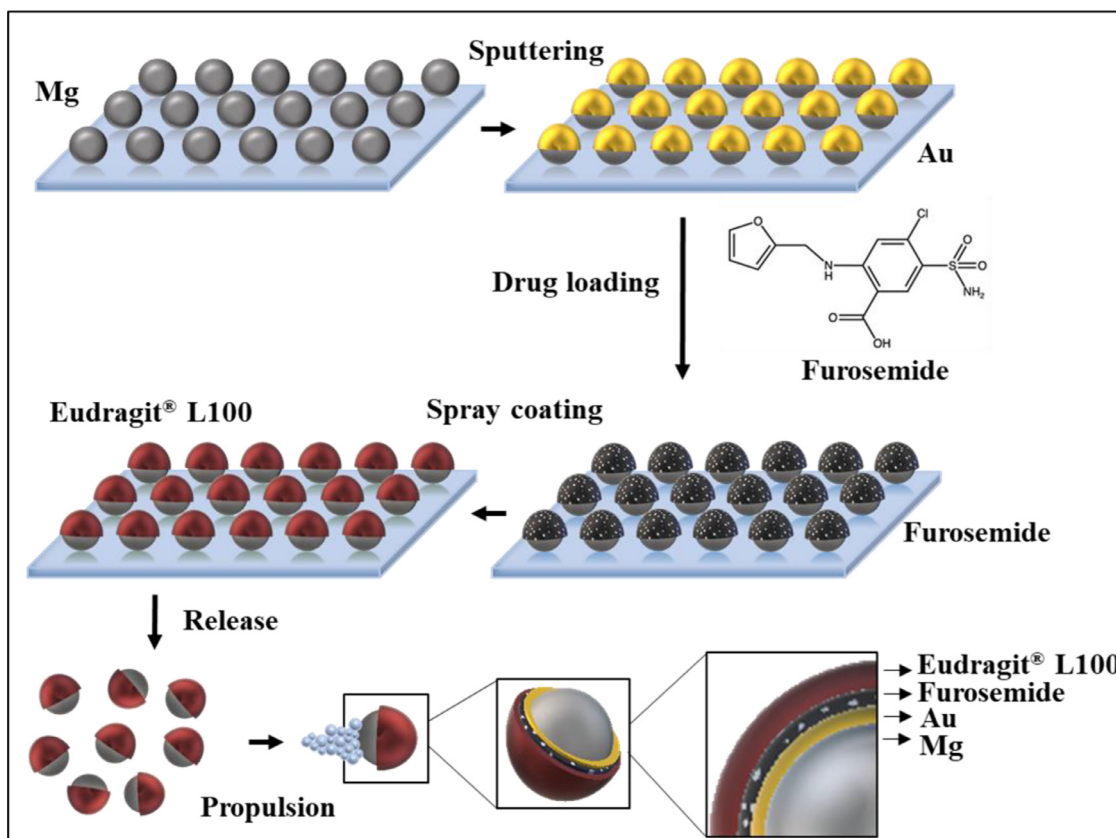
2.3. Characterization of micromotors

SEM TM3030Plus tabletop microscope (Hitachi, Japan) was used to visualize the Mg-based Janus micromotors during the fabrication process. Leica TCS SP8 CARS microscope (Leica, Germany) was used to confirm the presence of the drug on the Janus Mg-based micromotors. The system is equipped with a picoEmerald laser where the Stokes laser wavelength is fixed at 1032.4 nm, pump laser is tunable in the range 700–990 nm. Both lasers have a pulse duration of 2 ps with a repetition rate of 80 MHz. CARS images were carried out versus pump laser wavelength being tuned in the range that corresponds to the Raman shift between 2829.5 and 3250 cm⁻¹ with 27 excitation steps (1 nm step size). The microscope objective was 10 × 0.4 dry. Pump laser power and Stokes laser power were both set to 0.1 W. Forward CARS (F-CARS) signal collection geometry was used for CARS imaging. The Raman shift (wavenumber) is calculated from the following Eq. (1):

$$\text{Raman shift}[\text{cm}^{-1}] = \left(\frac{1}{\lambda_p [\text{nm}]} - \frac{1}{\lambda_s [\text{nm}]} \right) \times 10^7 \quad (1)$$

where λ_p (nm) is the excitation wavelength, and λ_s (nm) is the Raman spectrum wavelength.

Leica INM100 optical microscope coupled with a Nikon DS-Fi2 digital sight camera (Nikon, Japan) was used for size measurement and lifetime study measurements. Data were collected from 100



Scheme 1. Schematic representation of the fabrication process for the Mg-Au-Drug-Polymer micromotors.

independent measurements to obtain the average size. The lifetime study was performed for 20 different micromotors for each prepared type.

2.4. In vitro release of furosemide from Mg-based Janus micromotors

μ DISS Profiler™ (Pion, MA, USA) was used to determine the release of furosemide from Mg-Au Janus micromotors coated with Eudragit®. The drug release study was evaluated in 10 mL phosphate-buffered saline (PBS) (pH 7.4) and the control experiment was performed in a simulated stomach medium (pH 2.1). The experiments were carried out at 37 °C with a stirring rate of 100 rpm and the path length of the *in situ* UV probes of 5 mm. The PBS buffer was prepared by dissolving one PBS tablet (Sigma-Aldrich, USA) in 200 mL Milli-Q water (Merck Millipore, USA) using a magnetic stirrer for a few minutes. The simulated stomach medium was prepared by slowly adding 32% hydrochloric acid (HCl) to deionised (DI) water to adjust the pH value to 2.1. Before conducting the drug release experiments, a calibration curve was prepared for each experiment by the addition of different volumes of furosemide in a 10 mL of stock solution. The UV absorbance was measured in the range of 220–260 nm. The second derivative function was applied in the μ DISS software for the presentation of drug release to remove all appeared noises and interference during the experiment. The micromotors were dispersed on the quadratic piece of Si wafer which subsequently was attached to the clean magnetic stirrer that was subsequently placed at the bottom of a freshly cleaned μ DISS vessels. Finally, 10 mL of PBS solution was added to each vessel. UV measurements were carried out every 10 s and the total measurement time was 10 min (corresponding to full release of furosemide). The entire process was repeated for the simulated stomach medium and UV measurement was carried out for 65 min. *In vitro* experiment was performed in 3 replicates

for both pH conditions and therefore $n = 3$ denotes 3 samples with an ensemble-average readout of all particles.

2.5. Motion studies

The experiments for measuring the velocities of Mg-based micromotors were carried out in a solution containing 3 M NaCl (as a fuel) and 0.5 wt% Triton X-100 (as a surfactant). Leica INM100 optical microscope (Leica, Germany) connected to NIS Elements Software D version 4.20 was used for images and videos sequences. The velocity of the micromotors was analysed using ImageJ software version 1.53i (National Institutes of Health, USA). The videos were recorded and for each type of prepared micromotors, 40 measurements were performed.

3. Results and discussion

A multi-step asymmetric modification procedure was applied to fabricate Mg-based Janus micromotors. Commercially available Mg microspheres were used as a core of micromotors possessing susceptible effect to corrosion with an extremely low standard potential of -2.37 V. This characteristic plays an important role in this study, by forming the anodic part of an electrochemical reaction whereby the Mg microspheres easily oxidize [33]. First, Mg microspheres were dispersed on a glass slide and then a 40 nm thick Au layer was sputter-coated as an asymmetric spherical cap. Subsequently, the fabricated micromotors were loaded with furosemide. Finally, the drug-loaded Mg-Au micromotors were coated with Eudragit® L100 polymer by ultrasonic spray coating technique to provide drug protection. The ultrasonic spray coating is an entirely new technique when it comes to Mg-based spherical micromotors, and it is a technique that is highly scalable and reproducible which is important from a commercial point of view. Ultrasonic

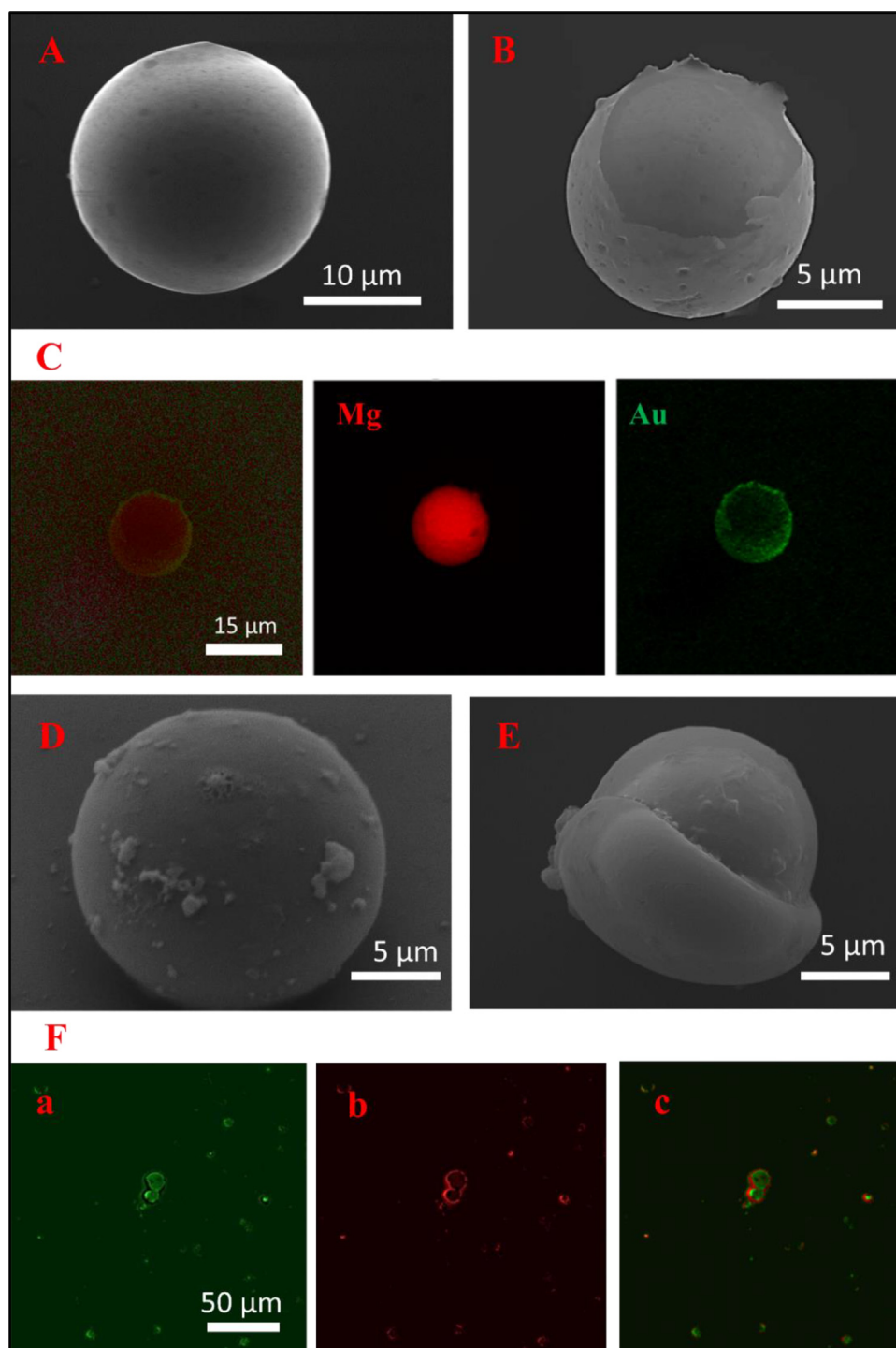


Fig. 1. Scanning electron microscopy (SEM) images of the surfaces of (A) bare Mg microparticle, (B) Mg coated with a thin Au layer (Mg-Au micromotor), (D) Mg-Au micromotor with furosemide on its surface (Mg-Au-Furo micromotor), (E) Mg-Au-Furo micromotor coated with Eudragit® (Mg-Au-Furo-Eudr micromotor), (C) energy dispersive X-ray spectroscopy (EDX) elemental mapping images of Mg-Au micromotors, (F) Coherent anti-Stokes Raman scattering (CARS) images of furosemide-loaded Mg-Au micromotors obtained in forward configuration (F-CARS) (a) F-CARS image at Raman shift 3150 cm^{-1} responsible for autofluorescence background of Mg-Au micromotors, (b) F-CARS image at Raman shift 3150 cm^{-1} responsible for furosemide, (c) merged autofluorescence and furosemide F-CARS images. Scales as indicated in respective images.

spray coating (a well-known coating method from, e.g., the semiconductor and PV industry) is renowned for making highly conformal coatings on 3D topographies and it allows for tuning the coating thickness with a high degree of precision [34]

Prepared micromotors are highly biocompatible as all used materials: magnesium, gold and Eudragit® L100 polymer coating are biocompatible. It is widely known that magnesium is an essential nutrient that the body needs for different physiological functions [35]. The gold have been frequently used in various biomedical ap-

plications such as bioimaging and anticancer drug delivery [36], while the Eudragit polymer coating has been extensively employed for controlled drug release [37]. Scheme 1 shows a schematic representation of the entire fabrication process for Mg-based micromotors and proof-of-concept applications for drug loading.

Autonomous propulsion was obtained by H_2 bubble recoil. Upon immersion in a 3 M NaCl solution, H_2 bubbles were generated, along with a magnesium hydroxide [$\text{Mg}(\text{OH})_2$] passivation layer [38]. This layer can interfere with the bubble generation pro-

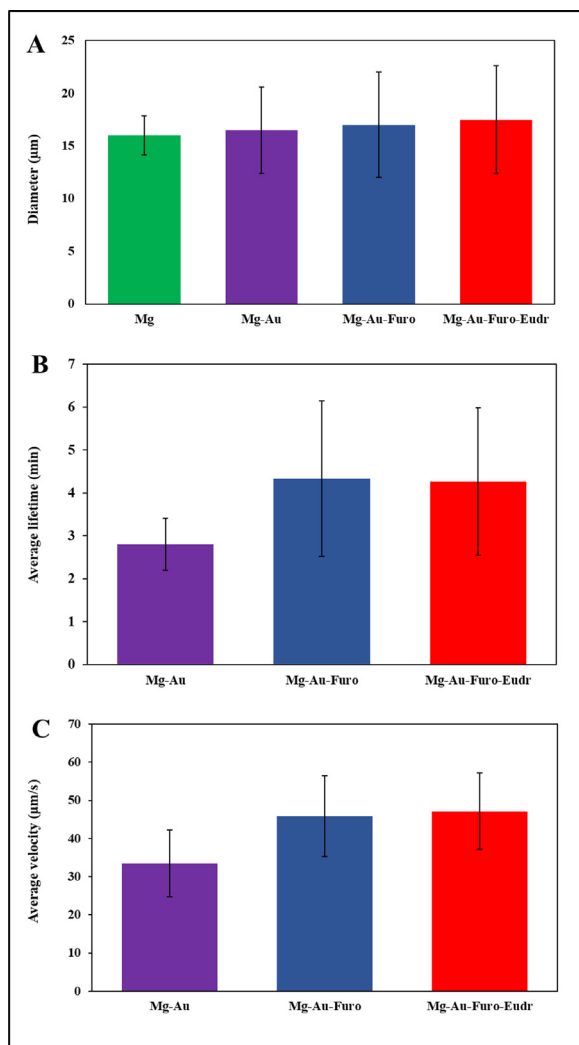


Fig. 2. (A) Average diameters of each prepared micromotor type obtained from analyzing 100 individual micromotors, (B) average lifetime of each prepared micromotor type, (C) average velocities of each prepared micromotor type. Experimental conditions: Room temperature, 3 M NaCl, 0.5 wt% Triton X-100. Error bars represent standard deviation ($n = 40$).

cess but the combination of pitting corrosion and macrogalvanic corrosion ensures that bubble generation can continue. Chloride ions (Cl^-) are well known for their ability to promote the pitting corrosion of magnesium in aqueous solutions [39]. The ions penetrate the $\text{Mg}(\text{OH})_2$ passivation layer where they subsequently balance the charge within the corrosion pits as the concentration of Mg^+ cations builds up [40]. The OH^- is depleted within the pit as the corrosion continues, which prevents passivation of the pit surface. When Mg^+ and Cl^- are accumulated, the pit environment becomes weakly acidic which further promotes Mg dissolution in the pit. The Au layer, deposited onto the Mg microparticles, plays a vital role in the macrogalvanic corrosion. When the micromotor is submerged in NaCl and both metals are in electrical contact, the $\text{Mg}(\text{OH})_2$ passivation layer corrodes preferentially to the Au layer.

Scanning electron microscopy (SEM) images were captured after each coating step to characterize the structure and surface morphology of the micromotors (Fig. 1). Fig. 1A shows the surface of the bare Mg microparticles, while Fig. 1B shows Mg microparticles after coating with Au. The difference in surface morphology of the particles before and after Au deposition in Fig. 1A and B is noticeable, confirming Janus formation with one Mg hemisphere coated with Au. Additionally, energy dispersive X-ray spectroscopy (EDX) data confirmed the presence of elements Mg and Au on micromo-

tors and verified the successful Janus distribution of Mg and Au on the particles (Fig. 1C).

Fig. 1(D and E) shows the surface morphology of the Mg-based Janus micromotors upon coating with furosemide and Eudragit® polymer. Additionally, it can be seen that the presence of drugs and polymer coatings does not disturb the spherical shape of the Mg microparticles. Comparing all the micrographs obtained, some speckles are visible on the surface (Fig. 1D). These speckles are assumed to be the corresponding drugs loaded onto the Mg-Au micromotors. It was noted that the drug concentration seems to vary between different micromotors. Two main factors influence the loading amount which are drug concentration and fabrication technique. Any significant changes to these factors can potentially alter the amount of drug loaded per micromotors. To improve drug loading uniformity, one should ideally develop and use furosemide formulations previously prepared with smaller and more uniform grain size. Besides that, the loading technique can be altered and optimized. Alternatively, micromotors solution and furosemide solution could be homogeneously mixed and shaken for a certain period to achieve maximum adsorption. From fundamental understanding, changing the concentration of the furosemide can also alter its distribution on the surface of the micromotors. In order to increase the drug loading amount, the concentration of furosemide could be increased. However, taking into account that usual furosemide initial dose is very small (only 40 mg) [41], it is not necessary to cover the whole hemisphere of micromotors with a large amount of furosemide.>

From Fig. 1E it is observed that micromotor coated with gastro-resistant lid - Eudragit® has asymmetric particle shape and that only one side of the particle grow in thickness.

Coherent anti-Stokes Raman scattering (CARS) microscopy imaging was performed for the first time to confirm that furosemide was successfully loaded onto the outer surface of the Mg-Au micromotors. This is a Raman based methods that uses two pulsed laser sources to chemically map the drug in a noninvasive and label-free manner. Another advantage of this system is the low solubility of furosemide in aqueous solution which allows for a long term detection of coated micromotors using CARS microscopy.

The resulting CARS microscopy images are presented in Fig. 1F. An autofluorescence background of Mg-Au micromotors at Raman shift 3150 cm^{-1} was obtained in forward configuration (F-CARS) and presented in Fig. 1Fa. Fig. 1Fb shows furosemide F-CARS image at Raman shift 3150 cm^{-1} . As can be seen in the merged images in Fig. 1Fc, drug (red color) is attached to the surface of the micromotors. The drug was found to have bounded to the fabricated Janus micromotors by physical adsorption in which the drugs are attached to the surface of micromotors through weak van der Waals forces. As expected, some drug is also present in between the micromotors, which indicates the importance of collecting and cleaning micromotors before conducting the drug release studies.

An optical microscope was used to measure the average diameter of each prepared type of micromotors by analyzing 100 individual micromotors. As it can be seen from the Fig. 2A, the sizes of the different micromotors do not appear distinctly different. Bare Mg particles are $16 \mu\text{m}$ in diameter, while the average size of the Mg-Au, Mg-Au-Furo and Mg-Au-Furo-Eudr micromotors are $16.5 \mu\text{m}$, $17 \mu\text{m}$ and $17.3 \mu\text{m}$, respectively. Based on these results, it can be concluded that coating does not have a significant impact on particle size distribution.

Next, a lifetime study was performed to explore how long the micromotors can generate bubbles before the fuel has been consumed. The experiments were conducted in solutions containing 3 M NaCl as fuel and 0.5 wt% Triton X-100 as a surfactant. Previous studies have shown an average lifetime of 1–6 min for Mg-based Janus micromotors [42,43]. It can be seen from the results presented in Fig. 2B that the average lifetimes of all prepared mi-

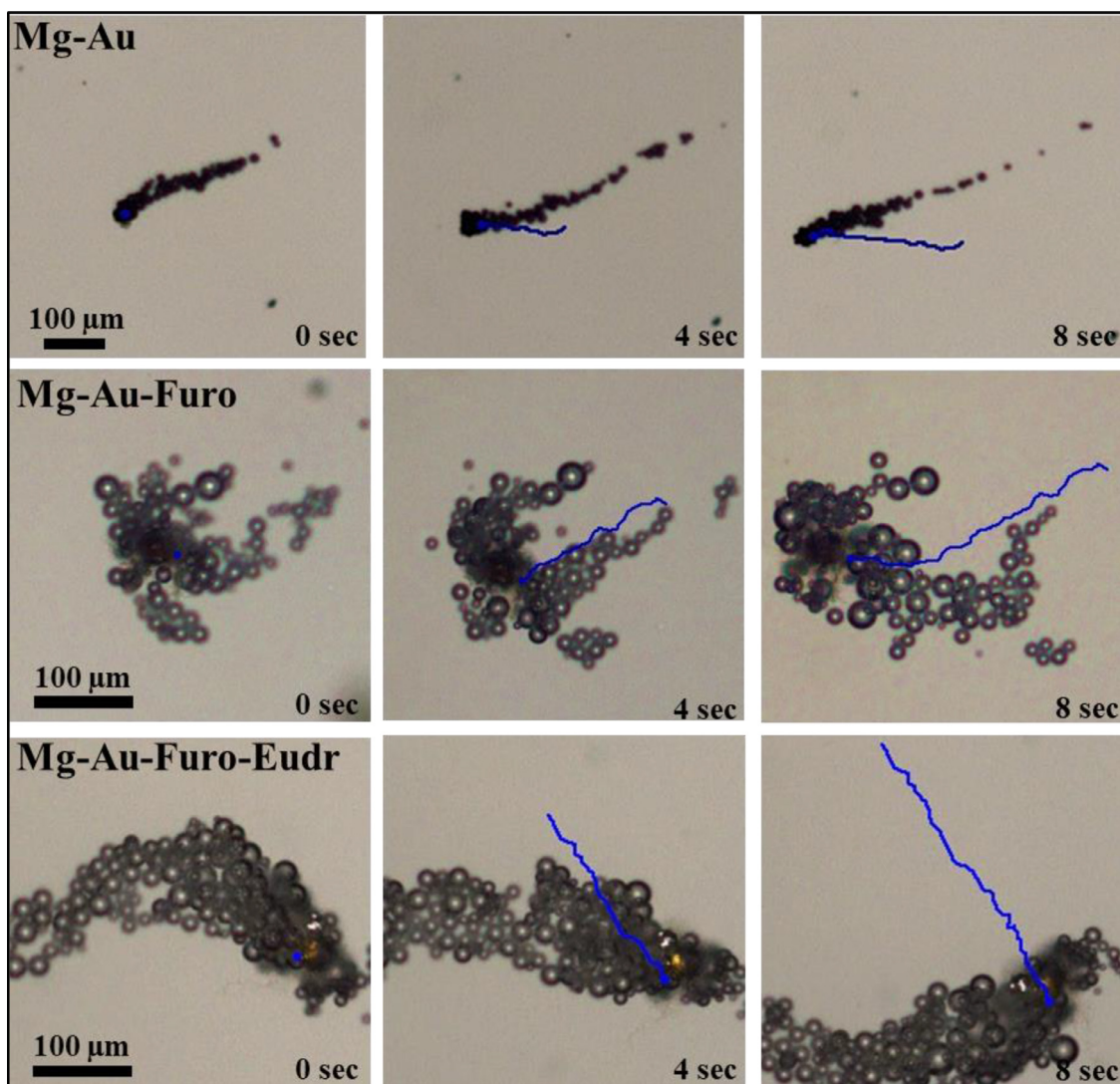


Fig. 3. Time-lapse tracking images of each prepared type of micromotors. The blue lines indicate the motion trajectories over a duration of 8 s with 4 s intervals. Experimental conditions: room temperature, 3 M NaCl, 0.5 wt% Triton X-100.

micromotors fall within the mentioned range. The plain Mg-Au micromotors exhibited the shortest lifetime (2.8 min). Similarly, to analyze the effect of the addition of the drug and polymer coating on the lifetime, Mg-Au micromotors are compared to Mg-Au-Furo and Mg-Au-Furo-Eudr micromotors. The Mg-Au-Furo and Mg-Au-Furo-Eudr micromotors have 54% and 50% higher lifetime than the Mg-Au micromotors, respectively. This claim is confirmed by statistical analysis, where the differences between the Mg-Au and Mg-Au-Furo micromotors (p -value = 0.0072) and between the Mg-Au and Mg-Au-Furo-Eudr micromotors (p -value = 0.0073) are both different and statistically significant. It can be concluded that the drug and Eudrigit polymer coating positively influence the lifetime of the micromotors. However, Mg-Au-Furo and Mg-Au-Furo-Eudr micromotors have a similar lifetime, 4.3 and 4.2 min, respectively (p -value = 0.3290). Due to the statistical insignificance between Mg-Au-Furo and Mg-Au-Furo-Eudr micromotors, it is not possible to determine if furosemide or polymer coating is more favorable in regard to the micromotor's lifetime.

Subsequently, we focused on studying the motion of the prepared Mg-based Janus micromotors (Fig. 2C). First, plain Mg-Au micromotors showed an average velocity of 33 μm/s. Control experiments with bare Mg particles were static. Comparing Mg-Au micromotors to Mg-Au-Furo and Mg-Au-Furo-Eudr, a rather large

difference in velocity is noticeable. The Mg-Au-Furo micromotors have 37% higher velocity than the Mg-Au micromotors, while the Mg-Au-Furo-Eudr micromotors were 41% faster than the Mg-Au micromotors. This claim is confirmed by statistical analysis, where the differences between the Mg-Au and Mg-Au-Furo micromotors (p -value = 0.0005) and between the Mg-Au and Mg-Au-Furo-Eudr micromotors (p -value = 0.0002) are both statistically significant. The average velocities of the micromotors with and without polymer coatings were also compared. However, the differences are not significant; Mg-Au-Furo-Eudr micromotors are only 3% faster than Mg-Au-Furo micromotors (p -value = 0.3742). This suggests that adding a drug compound on the surface of a micromotor can be beneficial for increasing the velocity. This might be caused by a nonuniform Au layer, in some locations exposing the Mg below. When coating with drug these exposed regions could then be partially covered which additionally facilitates more localized H₂ bubble generation, whereby the velocity would increase. Previously, studies have shown high velocity after coating of micromotors with polymer [44–47]. However, we do not see any additional significant effect of our enteric coating, probably because the surface is already fully covered by drug/Au.

The tracking and monitoring of the movement of each prepared micromotor type are shown in Fig. 3. The figure illustrates the

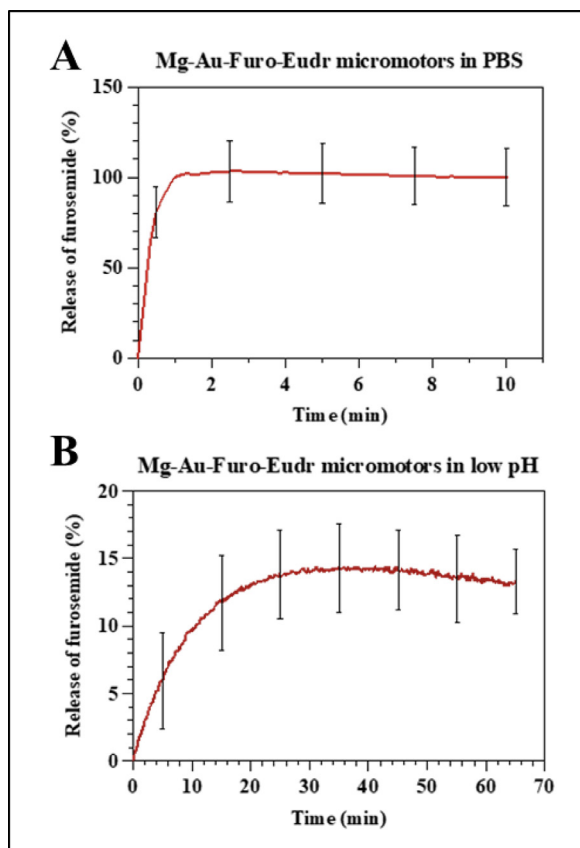


Fig. 4. *In vitro* release of furosemide from Mg-Au-Furo-Eudr micromotors as a function of time (A) in PBS (pH 7.4), and (B) in simulated stomach medium (pH 2.1). The data points are averages of three experiments.

propulsion of the micromotors in 3 M NaCl with 0.5 wt% Triton X-100 over a duration of 8 s. Linear trajectories were observed for a majority of the micromotors and only a few micromotors had a circular trajectory. The linear trajectories suggest a low Reynolds number ($Re \leq 10^{-3}$) since the non-linear (circular) motion transitions to linear motion at that particular Reynolds number [48]. Furthermore, the linear motion also suggests that the hydrodynamic drag and direction of the resultant force from the bubble propulsion did not change with time [49]. Faster moving micromotors create longer trajectories for the same time interval. The Mg-Au Janus micromotors have the smallest trajectories compared to the other two prepared micromotors which corresponds to the slowest velocity (Figs. 2C and 3).

To quantify the drug release from the micromotors, *in vitro* experiments were conducted using a μ DISS profilerTM. Release studies of Mg-Au Janus micromotors loaded with furosemide and coated with Eudragit[®] were carried out and presented in Fig. 4. It is apparent from Fig. 4A that furosemide is released immediately from Eudragit[®]-coated micromotors in PBS (pH 7.4). The results show that Eudragit[®] polymer coating successfully dissolved as expected since it is dissolvable above pH 6.0. Mg-Au-Furo-Eudr micromotors had fully released the drug in less than 3 min, proving that the micromotors are capable of super-fast drug release. By increasing the thickness of the polymer, it would be possible to delay the time of the drug release which would be beneficial if the micromotors are required to travel far in the GI tract before releasing the drug [29].

Since the Eudragit[®] polymer is only dissolvable at higher pH, a control release study in stomach medium (pH 2.1) was also conducted where little or no drug release was expected to happen.

Obtained data show that for micromotors coated with Eudragit[®] (Fig. 4B), 14% of the loaded drug was released in the stomach environment after 65 min. Possibly, a small amount of free drug was present between the micromotors, resulting in this small premature release. Another reason could be that the polymer coat is not completely covering the drug on the micromotors. An additional experiment was performed to measure the thickness of the polymer coating on the surface of the micromotors by contact stylus profilometry. The Eudragit[®] coating thickness was measured to be 527 nm which should be sufficient to uniformly cover the entire surface of the furosemide-loaded micromotors and provide adequate protection.

Based on the *in vitro* release profiles presented in Fig. 4, it is evident that the applied Eudragit[®] L100 coating serves as a protection for the drug in the stomach environment and ensures a complete and fast drug release in the intestinal environment.

4. Conclusion

In conclusion, we successfully loaded Mg-Au micromotors for the first time with furosemide. We demonstrated the possibility of using Eudragit[®] polymer coating for micromotor construction to achieve targeted furosemide release. The very first polymer deposition by ultrasonic spray coating technique was performed on Mg-Au-Furo micromotors to provide effective drug protection and pH-responsive drug release. We noted that Mg-Au-Furo-Eudr micromotors function as enterically coated self-propelled drug delivery devices. This conclusion is based on the performed *in vitro* release studies in acidic and neutral (PBS) chemical environments. The Mg-Au Janus micromotors are capable of loading furosemide and releasing the drug completely (100%) in a neutral pH medium within 3 min, after coating with Eudragit[®]. In acidic pH medium, a small amount of loaded furosemide was released (14%) after coating with Eudragit[®]. Presence of a pH sensitive layer on the surface of micromotors provides a great drug protection in acidic chemical environment and ensures a fast drug release in neutral chemical environment. Our data demonstrate that prepared Mg-Au Janus micromotors exhibit higher velocities after loading with furosemide or coating with pH sensitive polymer Eudragit[®]. Coherent anti-Stokes Raman scattering (CARS) microscopy imaging can be used for visualizing the halo-like drug distribution on the Mg spheres. While many techniques have shown promise in drug loading visualization, CARS imaging offers unique, rapid and label-free chemical imaging of drugs on the micromotors with the possibility of performing imaging in tissue and cell-cultures. Our future research will be directed towards targeted drug delivery using a dual microcontainers [50]-micromotor system which can be visualized via CARS microscopy.

Declaration of Competing Interest

The authors declare that they have no known competing financial interests or personal relationships that could have appeared to influence the work reported in this paper.

CRediT authorship contribution statement

Tijana Maric: Visualization, Writing – original draft, Writing – review & editing. **Sylvia Atladóttir:** Methodology, Investigation. **Lasse Højlund Eklund Thamdrup:** Methodology. **Oleksii Ilchenko:** Visualization. **Mahdi Ghavami:** Methodology. **Anja Boisen:** Supervision.

Acknowledgment

The authors would like to acknowledge the Danish National Research Foundation (DNRF122) and Villum Fonden (Grant No. 9301)

for Intelligent Drug Delivery and Sensing Using microcontainers and Nanomechanics (IDUN).

References

- [1] B. Sarmiento, S. Martins, D. Ferreira, E.B. Souto, Oral insulin delivery by means of solid lipid nanoparticles, *Int. J. Nanomed.* 2 (2007) 743–749.
- [2] N. Poonia, R. Kharb, V. Lather, D. Pandita, Nanostructured lipid carriers: versatile oral delivery vehicle, *Colloids Surfaces B Biointerfaces* 162 (2018) 236–245.
- [3] I. Gonçalves, P. Henriques, C. Seabra, M. Martins, The potential utility of chitosan micro/nanoparticles in the treatment of gastric infection, *Expert Rev. Anti Infect. Ther.* 12 (2014) 981–992.
- [4] M. Abdulkarim, P. Sharma, M.G. Reviews, Self-emulsifying drug delivery system: Mucus permeation and innovative quantification technologies, *Adv. Drug Deliv. Rev.* 142 (2019) 62–74.
- [5] X. Li, J. Qi, Y. Xie, X. Zhang, S. Hu, Y. Xu, Y. Lu, W. Wu, Nanoemulsions coated with alginate/chitosan as oral insulin delivery systems: preparation, characterization, and hypoglycemic effect in rats, *Int. J. Nanomed.* 8 (2013) 23–32.
- [6] M. Park, P. Balakrishnan, Polymeric nanocapsules with SEDDS oil-core for the controlled and enhanced oral absorption of cyclosporine, *Int. J. Pharm.* 441 (2013) 757–764.
- [7] Y. Yang, Y. Zhao, A. Yu, D. Sun, L.X. Yu, Oral drug absorption: Evaluation and prediction, *Dev. Solid Oral Dos. Forms Pharm. Theory Pract.* Second Ed. (2017) 331–354.
- [8] A. Sood, R. Panchagnula, Peroral route: An opportunity for protein and peptide drug delivery, *Chem. Rev.* 101 (2001) 3275–3303.
- [9] L.M. Ensign, R. Cone, J. Hanes, Oral drug delivery with polymeric nanoparticles: The gastrointestinal mucus barriers, *Adv. Drug Deliv. Rev.* 64 (2012) 557–570.
- [10] L. Zhang, S. Wang, M. Zhang, J. Sun, Nanocarriers for oral drug delivery, *J. Drug Target.* 21 (2013) 515–527.
- [11] X. Zhou, X. Huang, B. Wang, L. Tan, Y. Zhang, Y. Jiao, Light/gas cascade-propelled Janus micromotors that actively overcome sequential and multi-staged biological barriers for precise drug delivery, *Chem. Eng. J.* 408 (2021) 127897.
- [12] K. Yuan, Z. Jiang, B. Jurado-Sánchez, A. Escarpa, Nano/micromotors for diagnosis and therapy of cancer and infectious diseases, *Chem. A Eur. J.* 26 (2020) 2309–2326.
- [13] J. Li, B. de Ávila, W. Gao, L. Zhang, Micro/nanorobots for biomedicine: delivery, surgery, sensing, and detoxification, *Sci. Robot.* 2 (2017) eaam6431.
- [14] C. Chen, E. Karshalev, J. Guan, J. Wang, Magnesium-based micromotors: Water-powered propulsion, multifunctionality, and biomedical and environmental applications, *Small.* 14 (2018) 1–10.
- [15] G. Tang, L. Chen, L. Lian, F. Li, H. Ravanbakhsh, M. Wang, Y.S. Zhang, C. Huang, Designable dual-power micromotors fabricated from a biocompatible gas-hearing strategy, *Chem. Eng. J.* 407 (2021) 127187.
- [16] C. Xu, S. Wang, H. Wang, K. Liu, S. Zhang, B. Chen, H. Liu, F. Tong, F. Peng, Y. Tu, Y. Li, Magnesium-based micromotors as hydrogen generators for precise rheumatoid arthritis therapy, *Nano Lett.* 21 (2021) 1982–1991.
- [17] P. Mayorga-Burrezo, C.C. Mayorga-Martinez, M. Pumera, Light-driven micromotors to dissociate protein aggregates that cause neurodegenerative diseases, *Adv. Funct. Mater.* (2021) 2106699.
- [18] W. Gao, R. Dong, S. Thamphiwatana, J. Li, W. Gao, L. Zhang, J. Wang, Artificial micromotors in the mouse's stomach: A step toward in vivo use of synthetic motors, *ACS Nano* 9 (2015) 117–123.
- [19] T. Maric, M.Z.M. Nasir, N.F. Rosli, M. Budanović, R.D. Webster, N.J. Cho, M. Pumera, Microrobots derived from variety plant pollen grains for efficient environmental clean up and as an anti-cancer drug carrier, *Adv. Funct. Mater.* 30 (2020) 200011225.
- [20] B.E.F. De Ávila, P. Angsantikul, J. Li, M. Angel Lopez-Ramirez, D.E. Ramirez-Herrera, S. Thamphiwatana, C. Chen, J. Delezuk, R. Samakapiruk, V. Ramez, L. Zhang, J. Wang, Micromotor-enabled active drug delivery for in vivo treatment of stomach infection, *Nat. Commun.* 8 (2017) 1–8.
- [21] E. Gultepe, J.S. Randhawa, S. Kadam, S. Yamanaka, F.M. Selaru, E.J. Shin, A.N. Kallou, D.H. Gracias, Biopsy with thermally-responsive untethered microtools, *Adv. Mater.* 25 (2013) 514–519.
- [22] A. Hortelão, R. Carrascosa, N.M.C. Nano, Targeting 3D bladder cancer spheroids with urease-powered nanomotors, *ACS Nano* 13 (2018) 429–439.
- [23] J. Wang, Self-propelled affinity biosensors: Moving the receptor around the sample, *Biosens. Bioelectron.* 76 (2016) 234–242.
- [24] X. Yan, Q. Zhou, M. Vincent, Y. Deng, J. Yu, J. Xu, T. Xu, T. Tang, L. Bian, Y.X.J. Wang, K. Kostarelos, L. Zhang, Multifunctional biohybrid magnetite microrobots for imaging-guided therapy, *Sci. Robot.* 2 (2017) eaaq1155.
- [25] S. Balasubramanian, D. Kagan, C.M.J. Hu, S. Campuzano, M.J. Lobo-Castañón, N. Lim, D.Y. Kang, M. Zimmerman, L. Zhang, J. Wang, Micromachine-enabled capture and isolation of cancer cells in complex media, *Angew. Chem.* 123 (2011) 4247–4250.
- [26] S. Sattayasamitsathit, H. Kou, W. Gao, W. Thavarajah, K. Kaufmann, L. Zhang, J. Wang, Fully loaded micromotors for combinatorial delivery and autonomous release of cargoes, *Small.* 10 (2014) 2830–2833.
- [27] J. Wu, S. Ma, M. Li, X. Hu, N. Jiao, S. Tung, L. Liu, Enzymatic/magnetic hybrid micromotors for synergistic anticancer therapy, *ACS Appl. Mater. Interfaces* 13 (2021) 31514–31526.
- [28] H. Zhu, J. Huang, H. Chen, X. Feng, MOF-derived magnetic Co@porous carbon as a direction-controlled micromotor for drug delivery, *New J. Chem.* 44 (2020) 21085–21091.
- [29] J. Li, S. Thamphiwatana, W. Liu, B.E.F. de Ávila, P. Angsantikul, E. Sandraz, J. Wang, T. Xu, F. Soto, V. Ramez, X. Wang, W. Gao, L. Zhang, J. Wang, Enteric micromotor can selectively position and spontaneously propel in the gastrointestinal tract, *ACS Nano* 10 (2016) 9536–9542.
- [30] L.L. Boles Ponto, R.D. Schoenwald, Furosemide (frusemide) a pharmacokinetic/pharmacodynamic review (part I), *Clin. Pharmacokinet.* 18 (2012) 381–408.
- [31] L.H. Nielsen, A. Meleró, S.S. Keller, J. Jacobsen, T. Garrigues, T. Rades, A. Müllertz, A. Boisen, Polymeric microcontainers improve oral bioavailability of furosemide, *Int. J. Pharm.* 504 (2016) 98–109.
- [32] G.E. Granero, M.R. Longhi, M.J. Mora, H.E. Junginger, K.K. Midha, V.P. Shah, S. Stavchansky, J.B. Dressman, D.M. Barends, Biowaiver monographs for immediate release solid oral dosage forms: Furosemide, *J. Pharm. Sci.* 99 (2010) 2544–2556.
- [33] M. Matsui, Study on electrochemically deposited Mg metal, *J. Power Sources* 196 (2011) 7048–7055.
- [34] S. Bose, S.S. Keller, T.S. Alstrøm, A. Boisen, K. Almdal, Process optimization of ultrasonic spray coating of polymer films, *Langmuir* 29 (2013) 6911–6919.
- [35] J. Vormann, Magnesium: nutrition and metabolism, *Mol. Asp. Med.* 24 (2003) 27–37.
- [36] S.D. Brown, P. Nativo, J.A. Smith, D. Stirling, P.R. Edwards, B. Venugopal, D.J. Flint, J.A. Plumb, D. Graham, N.J. Wheate, Gold nanoparticles for the improved anticancer drug delivery of the active component of oxaliplatin, *J. Am. Chem. Soc.* 132 (2010) 4678–4684.
- [37] C. Wu, J.W. McGinity, Influence of an enteric polymer on drug release rates of theophylline from pellets coated with Eudragit® RS 30D, *Pharm. Dev. Technol.* 8 (2003) 103–110.
- [38] L. Kong, N.F. Rosli, H.L. Chia, J. Guan, M. Pumera, Self-propelled autonomous Mg/Pt Janus micromotor interaction with human cells, *Bull. Chem. Soc. Jpn.* 92 (2019) 1754–1758.
- [39] C. Chen, E. Karshalev, J. Guan, J. Wang, Magnesium-based micromotors: Water-powered propulsion, multifunctionality, and biomedical and environmental applications, *Small* 14 (2018) 1704252.
- [40] W. Gao, X. Feng, A. Pei, Y. Gu, J. Li, J. Wang, Seawater-driven magnesium based Janus micromotors for environmental remediation, *Nanoscale* 5 (2013) 4696–4700.
- [41] D.C. Brater, P. Chennavasin, R. Seiwel, Furosemide in patients with heart failure: Shift in dose-response curves, *Clin. Pharmacol. Ther.* 28 (1980) 182–186.
- [42] F. Mou, C. Chen, H. Ma, Y. Yin, Q. Wu, J. Guan, Self-propelled micromotors driven by the magnesium–water reaction and their hemolytic properties, *Angew. Chem. Int. Ed.* 52 (2013) 7208–7212.
- [43] F. Mou, C. Chen, Q. Zhong, Y. Yin, H. Ma, J. Guan, Autonomous motion and temperature-controlled drug delivery of Mg/Pt-Poly(N-isopropylacrylamide) Janus micromotors driven by simulated body fluid and Blood Plasma, *ACS Appl. Mater. Interfaces* 6 (2014) 9897–9903.
- [44] J. Wang, B.J. Toebes, A.S. Plachokova, Q. Liu, D. Deng, J.A. Jansen, F. Yang, D.A. Wilson, Self-propelled PLGA micromotor with chemotactic response to inflammation, *Adv. Healthc. Mater.* 9 (2020) 1901710.
- [45] B. Jurado-Sánchez, M. Pacheco, R. Maria-Hormigos, A. Escarpa, Perspectives on Janus micromotors: Materials and applications, *Appl. Mater. Today* 9 (2017) 407–418.
- [46] F. Mou, C. Chen, Q. Zhong, Y. Yin, H. Ma, J. Guan, Autonomous motion and temperature-controlled drug delivery of Mg/Pt-poly(n-isopropylacrylamide) Janus micromotors driven by simulated body fluid and blood plasma, *ACS Appl. Mater. Interfaces* 6 (2014) 9897–9903.
- [47] L. Wang, J. Chen, X. Feng, W. Zeng, R. Liu, Xiujing Lin, Y. Ma, L. Wang, Self-propelled manganese oxide-based catalytic micromotors for drug delivery, *RSC Adv.* 6 (2016) 65624–65630.
- [48] G. Zhao, N.T. Nguyen, M. Pumera, Reynolds numbers influence the directionality of self-propelled microjet engines in the 10^{-4} regime, *Nanoscale* 5 (2013) 7277–7283.
- [49] F. Mou, C. Chen, H. Ma, Y. Yin, Q. Wu, J. Guan, Self-propelled micromotors driven by the magnesium–water reaction and their hemolytic properties, *Angew. Chem. Int. Ed.* 52 (2013) 7208–7212.
- [50] C. Mazzoni, F. Tentor, S.A. Strindberg, L.H. Nielsen, S.S. Keller, T.S. Alstrøm, C. Gundlach, A. Müllertz, P. Marizza, A. Boisen, From concept to in vivo testing: Microcontainers for oral drug delivery, *J. Control. Release* 268 (2017) 343–351.